ELSEVIER

1359-8368(95)00031-3

Composites: Part B **27B** (1996) 275–284

1359-8368/96/$15.00

Effect of fiber diameter variation on properties of cement-based matrix fiber reinforced composites

Victor C. Li and Karthikeyan Obla
Advanced Civil Engineering Materials Research Laboratory, Department of Civil and Environmental Engineering, University of Michigan, Ann Arbor, MI 48109-2125, USA
(Received January 1995; accepted May 1995)

Depending on process route, fibers for composite reinforcement typically have some degree of variation in diameter. This paper examines the effect of varying fiber diameter on properties of cement-based matrix composites such as first crack strength, fracture energy, and ultimate tensile strength. The analytical development of fiber bridging action across matrix cracks accounts for fibers that pull-out and fibers which rupture. Model calculations reveal that within reasonable limits, composite properties should not decay due to fiber diameter variations.

(Keywords: composite; fiber diameter; quality control; first crack strength; fracture energy; ultimate tensile strength)

INTRODUCTION

The fundamental constitutive relationship that describes the post cracking composite properties is the bridging stress (σ_B) versus crack opening (δ) relationship. This relationship quantifies the non-linear spring-like behavior of fibers bridging across a matrix crack. Many important composite properties such as the first crack strength, fracture energy, and the ultimate tensile strength can be derived from this σ_B–δ relationship[1–3]. The σ_B–δ relationship associated with fiber pullout and pullout/breakage have been investigated and complete closed form analytic solutions are available for discontinuous random fiber reinforced brittle matrix composites[1,4]. These studies have been carried out for fibers of uniform diameter only.

In the present work, the additional effect of fiber diameter variation is analyzed. Fiber diameter is assumed to vary according to a prescribed probability distribution and this effect is incorporated in the above-mentioned studies. The case of varying fiber diameter is then compared with that of constant mean fiber diameter in order to determine the influence of fiber diameter variation on composite properties. Separate expressions are derived for the model assuming all fibers pulled out and the model for which fiber rupture is considered. In the following section, the general formulation of the fundamental σ_B–δ relationship and representation of fiber diameter variation assumed in this study is first presented.

σ_B–δ FORMULATION AND FIBER DIAMETER DISTRIBUTION

For a discontinuous random fiber composite with varying fiber diameter, the composite σ_B–δ relationship can be predicted by integrating over the contributions of the individual fibers which bridge a matrix crack plane perpendicular to the loading axis. The fiber embedment length is assumed to vary according to a uniform distribution from 0 to $L_f/2$ and the orientation angle is assumed to vary from 0 to $\pi/2$ according to 3D uniform randomness. Following Li *et al.*[5], the σ_B–δ relationship can be calculated as:

$$\sigma_B(\delta) = \frac{4V_f}{\pi}\int_{d_1}^{d_2}\int_0^{\pi/2}\int_0^{(L_f/2)\cos\phi}\frac{1}{d_f^2} \times P(\delta;\phi)p_1(d_f)p_2(\phi)p_3(z)\mathrm{d}z\,\mathrm{d}\phi\,\mathrm{d}d_f \quad (1)$$

where $P(\delta;\phi)$ is the load–displacement relationship of a single fiber pulled out of the matrix (equation (A1)), d_1 and d_2 are the smallest and largest fiber diameters, $p_1(d_f)$ is the probability density function for the fiber diameter, $p_2(\phi)$ and $p_3(z)$ are probability density functions of the orientation angle ϕ and centroidal distance z of fibers from the crack plane defined as follows:

$$p_2(\phi) = \sin\phi \qquad \text{for } 0 \le \phi \le \frac{\pi}{2} \quad (2)$$

$$p_3(z) = 2/L_f \qquad \text{for } 0 < z < (L_f/2) \quad (3)$$

In the present investigation, the fiber diameter has

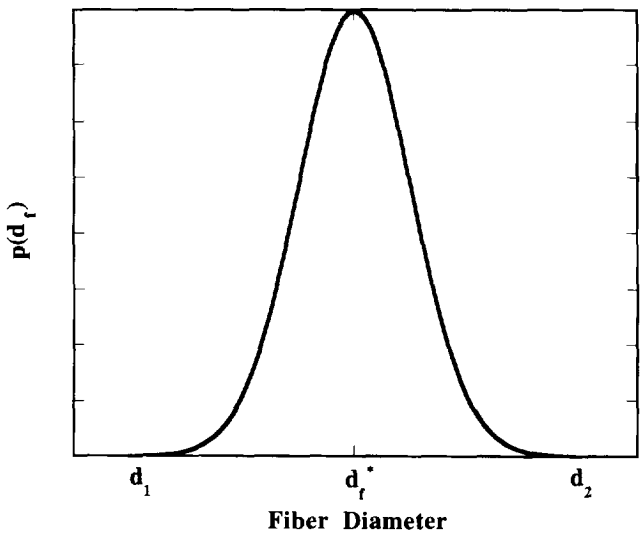

Figure 1 Fiber diameter distribution described as a normal probability density function

been assumed to vary according to a normal probability distribution (see *Figure 1*):

$$p_1(d_f) = \frac{1}{\sigma\sqrt{2\pi}} e^{-\left((d_f - d_f^*)^2/2\sigma^2\right)} \tag{4}$$

where d_f^* = mean fiber diameter. This form has been used in equation (1) in all calculations presented in this paper.

In order to find the maximum value of standard deviation (σ) at which the fiber diameter can be normally distributed for the particular d_f^*, d_1 and d_2 chosen, the following procedure was adopted. It is well known that 99.97% of the area of a normal probability distribution curve can be described within $\pm 3\sigma$ from the mean fiber diameter. Then σ can be evaluated by equating the difference between the smallest (d_1) and mean fiber diameter (d_f^*) to 3σ.

Actual fiber diameter variation depends upon fiber type and manufacture route, and is usually less than ±30%, more typically ±15%[6]. Brown[6] measured the diameter of glass fibers for composite reinforcements and his results indicate that the fiber diameter lies in the range ±15% from the mean fiber diameter. Further, the variation was found to be properly described by a normal probability density function. Unless otherwise specified, for numerical results presented in this paper, the diameter variation is assumed to be within ±30% of the mean diameter (d_f^*). For $d_f^* = 10\,\mu$m, based on the procedure described above, we have $d_1 = 7\,\mu$m, $d_2 = 13\,\mu$m and $\sigma = 1$. The more general analytical expressions derived can be applied to other magnitudes of fiber diameter variations.

FIBER PULLOUT CASE

This section is valid for those fibers short enough to pull-out. This means that fibers are of a length less than twice the critical embedment length, L_c, defined as:

$$L_c = \frac{d_f \sigma_{fu}}{4\tau} \tag{5}$$

For thin flexible fibers which bridge a matrix crack at an inclined angle, Li *et al.*[7] found experimentally that the bridging stress increases as a function of the inclination angle. Conceptually, the fiber acts like a flexible rope passing over a friction pulley. This effect is captured simply by the Euler friction law containing the snubbing coefficient, f. The resulting increase in bridging stress in the fibers reduces the critical embedment length L_c, to $L_c e^{-f\pi/2}$, where $\pi/2$ in the exponent refers to the maximum angle of fiber inclination (to the normal of the matrix crack). In this section, therefore, all analyses are carried out for short fibers with length given by:

$$L_f < 2L_c e^{-f\pi/2} \tag{6}$$

Comparison of composite properties for the case of uniform fiber diameter should be done with the fiber pullout model (FPM) established by Li[1].

Prepeak σ_B–δ relationship

Using equations (2), (3), (4) and (A1) in equation (1), the prepeak σ_B–δ relationship in normalized form for the case of varying fiber diameter can be derived (Appendix 2) as:

$$\tilde{\sigma}_B(\tilde{\delta}) = \begin{cases} g[2(\tilde{\delta}/\tilde{\delta}^*)^{1/2} h(z_1, z_2)] - \tilde{\delta}/\tilde{\delta}^* & \text{for } \tilde{\delta} \le \tilde{\delta}_2 \quad (7a) \\ g[2(\tilde{\delta}/\tilde{\delta}^*)^{1/2} h(z_1, z_3) - \tilde{\delta}/\tilde{\delta}^* + (1-\tilde{\delta})^2 k(z_3, z_2)] & \text{for } \tilde{\delta}_2 \le \tilde{\delta} \le \tilde{\delta}_1 \quad (7b) \end{cases}$$

where parameter normalizations are as given in Appendix 1 and $\tilde{\delta}_i = 2(\tau/E_f)(L_f/d_i)$.

The $h(z_i, z_j)$ and $k(z_i, z_j)$ functions are defined as:

$$h(z_i, z_j) = (1/\sqrt{2\pi}) \int_{z_i}^{z_j} [1 + (\sigma z/d_f^*)]^{-1/2} e^{-z^2/2} dz$$

$$k(z_i, z_j) = (1/\sqrt{2\pi}) \int_{z_i}^{z_j} [1 + (\sigma z/d_f^*)]^{-1} e^{-z^2/2} dz$$

are modifer terms which account for the fiber diameter variation in terms of

$$z_i = \begin{cases} (d_i - d_f^*)/\sigma & i = 1, 2 \\ [(2\tau L_f/E_f\tilde{\delta}) - d_f^*]/\sigma & i = 3 \end{cases}$$

All other terms in equation (7) are defined in Appendix 1.

Figure 2 shows the prepeak σ_B–δ relationship. It can be seen that there is a slight increase (<0.75%) in the bridging stress for the composite containing varying fiber diameter as compared to that reinforced with fibers of uniform diameter only.

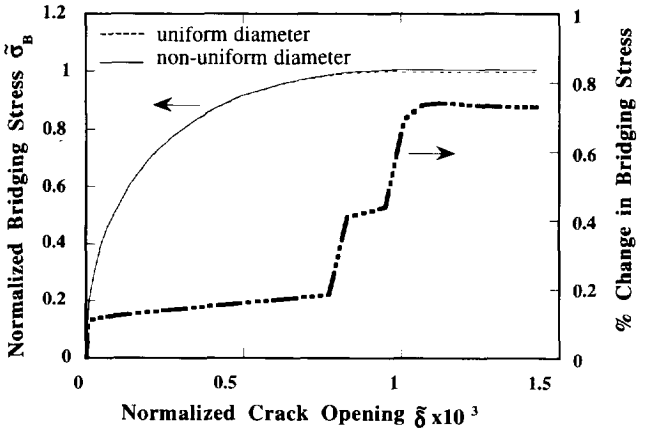

Figure 2 Influence of fiber diameter variation on the prepeak σ_B–δ relationship

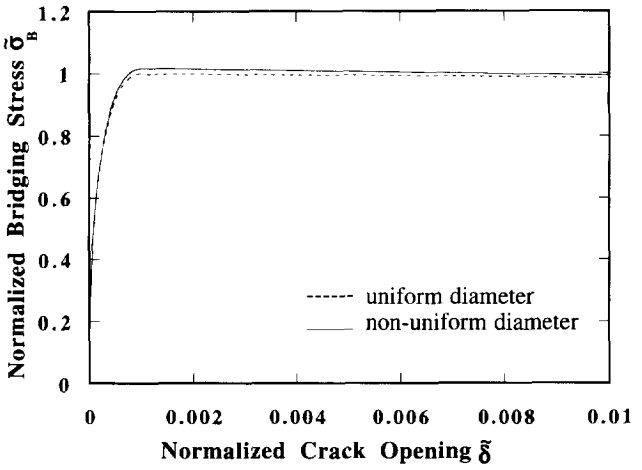

Figure 4 Influence of fiber diameter variation on complete σ_B–δ relationship

Post-peak σ_B–δ relationship

The post-peak σ_B–δ relationship is evaluated in the same manner as for the prepeak σ_B–δ relationship except that $\tilde{\delta} > \tilde{\delta}_1$ corresponding to the crack-opening when all fibers have been fully debonded. The result is

$$\tilde{\sigma}_B(\tilde{\delta}) = g(1-\tilde{\delta})^2 k(z_1, z_2) \quad \text{for } 1 \geq \tilde{\delta} \geq \tilde{\delta}_1 \qquad (8)$$

Figure 3 compares the post-peak σ_B–σ relationship between composites containing uniform diameter fibers and that containing variable diameter fibers. As before there is a slight increase (about 0.75%) in the bridging stress of the composite containing varying fiber diameter, as compared to that reinforced with fibers of uniform diameter only.

Figure 4 shows the complete bridging-stress versus crack-opening relationship. This figure highlights the fact that even at the transition region between the prepeak and the post-peak part of the σ_B–δ relationship, there is a negligible difference between the bridging stresses predicted for the uniform and non-uniform fiber diameter cases.

The above results indicate that the σ_B–δ relationship for discontinuous random fiber composites is not sensitive to variation in fiber diameter. This conclusion is found to hold even for composites with larger standard deviation (accompanied by larger mean diameter). This conclusion further suggests that other composite properties directly associated with the σ_B–δ relationship are likewise insensitive to fiber diameter variation, as is demonstrated below.

Composite fracture energy

Fracture energy is defined as the energy absorbed for unit area of crack advancement. For a fiber composite with fiber pullout in the crack wake as the dominant energy absorption mechanism, its fracture energy may be interpreted as[1,8]:

$$G_c = \int_0^{L_f/2} \sigma_B(\delta)\mathrm{d}\delta \qquad (9)$$

where σ_B is the cohesive stress contributed by fiber bridging.

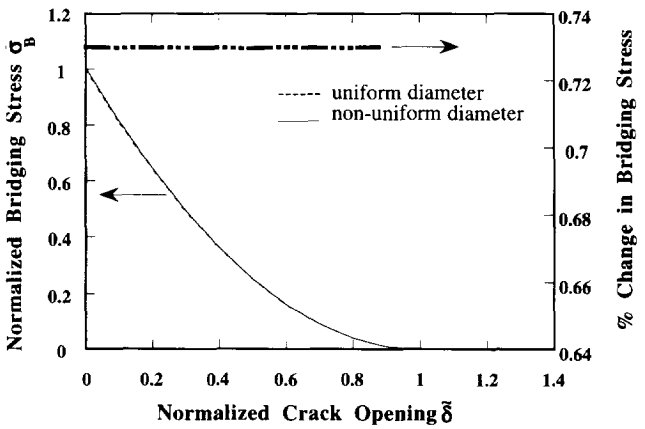

Figure 3 Influence of fiber diameter variation on the postpeak σ_B–δ relationship

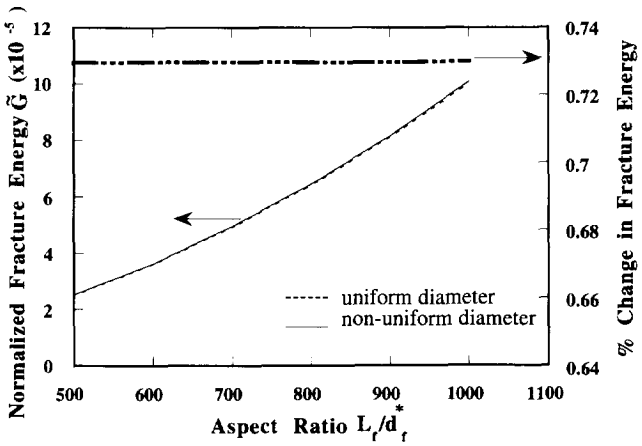

Figure 5 Influence of fiber diameter variation on fracture energy of a composite with increasing fiber lengths

Using equation (1) in equation (9), it can be shown that:

$$G_c = \frac{1}{12} g\tau V_f d_f^* \left(\frac{L_f}{d_f^*}\right)^2 k(z_1, z_2) \qquad (10)$$

where g, τ are defined in Appendix 1.

Figure 5 shows the composite fracture energy versus fiber aspect ratio. As expected the composite with fiber diameter variation shows slightly improved properties. Note that in this figure

$$\tilde{G} = \frac{G_c}{\frac{1}{12} g\tau V_f d_f^* \left(\frac{L_f}{d_f^*}\right)^2}$$

Composite first crack strength

The first crack strength, σ_{fc}, is the applied tensile stress at which a matrix crack first spreads throughout a cross-section of a composite loaded in tension. Based on the fracture mechanics approach, Li and Leung[2] treated the bridging action of fibers as the cohesive traction acting across the crack flanks. A brief summary of derivation of σ_{fc} for the composites with uniform fiber diameter can be found in Appendix 1.

For the case of varying fiber diameter, the first crack strength is derived in Appendix 2, resulting in:

$$\frac{\tilde{\sigma}_{fc}}{g} = \begin{cases} \dfrac{\sqrt{\pi}}{2}\dfrac{\bar{K}}{\bar{c}} - \dfrac{\bar{c}}{2} + \dfrac{4}{3}\sqrt{\bar{c}}\, h(z_1, z_2) & \bar{c} \le \dfrac{d_f^*}{d_2} \qquad (11a) \\ \dfrac{\sqrt{\pi}}{2}\dfrac{\bar{K}}{\bar{c}} + \displaystyle\int_0^a f(\bar{c}, R) h(z_1, z_3) \mathrm{d}R - \frac{1}{\sqrt{2\pi}} \int_0^a \int_{z_1}^{z_3} (\bar{c}R) e^{-z^2/2} \mathrm{d}z\, \mathrm{d}R & \dfrac{d_f^*}{d_2} \le \bar{c} \le \dfrac{d_f^*}{d_1} \qquad (11b) \\ \quad + \displaystyle\int_0^a \frac{R}{\sqrt{1-R^2}} k(z_3, z_2) \mathrm{d}R + h(z_1, z_2) \int_a^1 f(\bar{c}, R) \mathrm{d}R - \frac{\bar{c}}{2}(1 - a^2) & \end{cases}$$

where $a = [1 - (d_f^*/d_2\bar{c})^2]^{1/2}$, $f(\bar{c}, R) = 2\bar{c}^{1/2} R/(1 - R^2)^{1/4}$ and R is a normalized radial distance measured from the center ($R = 0$) of a penny-shaped crack. $\bar{c}$ and $\bar{K}$ are normalized crack radius and matrix toughness, respectively, defined in Appendix 1.

Figure 6 shows the first crack strength versus crack size for the uniform and non-uniform diameter cases. As before the variable fiber diameter case shows a slight increase (about 1.3%) in first crack strength for all crack sizes.

FIBER PULL-OUT/RUPTURE CASE

When fibers are long, it is possible for bridging fibers with long embedment lengths to break by tensile rupture instead of pullout. In this case some fibers will break while others will pull-out. As a result, the shape of the σ_B–δ curve will be affected. When fibers have variable diameter, it is conceivable that those with smaller diameters will tend to break first. In this section, the

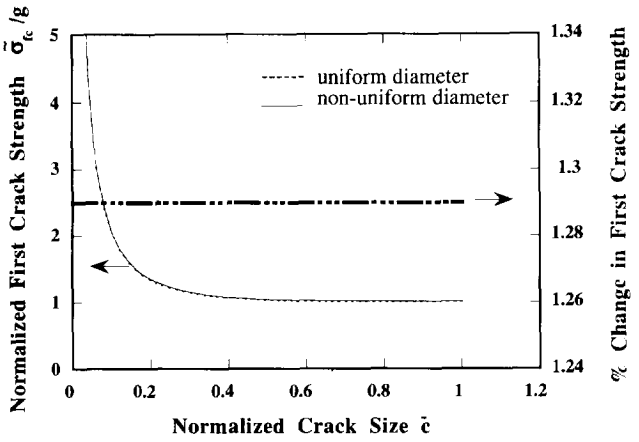

Figure 6 Influence of fiber diameter variation on first crack strength of composite, as a function of flaw size

σ_B–δ relationship and associated composite properties are investigated for their sensitivity to fiber diameter variation. For this case, fibers are assumed to have a length of $L_f > 2L_c e^{-f\pi/2}$. Comparison of composite properties with the case of uniform fiber diameter should be performed with the fiber pull-out/rupture model (FPRM) established by Maalej *et al.*[4].

If one were to use the fiber pull-out model (FPM) for the case of $L_f > 2L_c e^{-f\pi/2}$ the results could be quite erroneous. This aspect is shown in *Figure 7* which shows

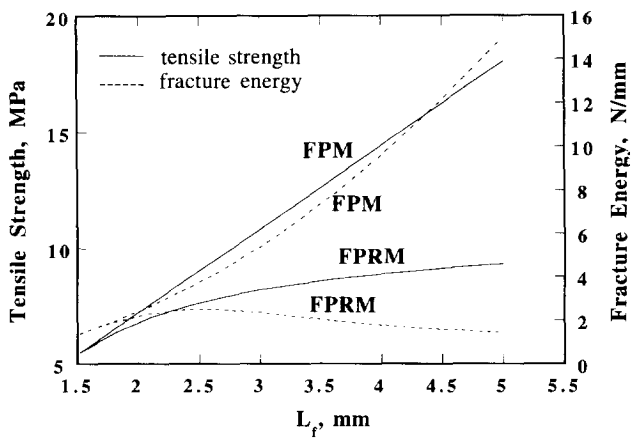

Figure 7 Tensile strength and fracture energy predictions from FPRM and FPM. Note loss of strength and fracture energy due to fiber rupture

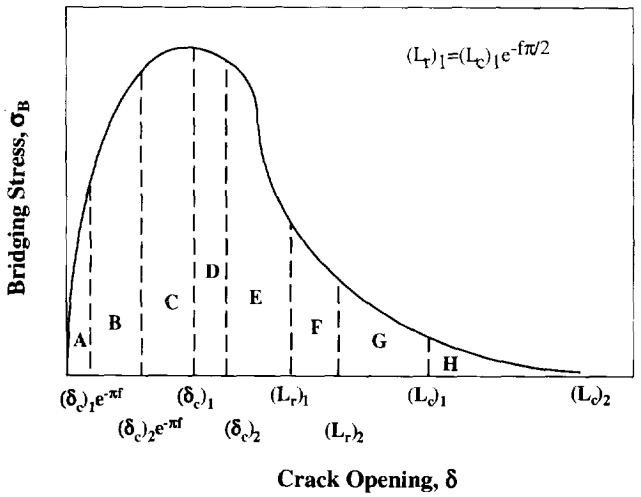

Figure 8 Schematic σ_b–δ relationship for composites with variable fiber diameter, and with fiber rupture. Sectors indicated correspond to crack openings within which groups of fibers rupture or pull-out. See text for more details. $(L_r)_1 = (L_c)_1 e^{-f\pi/2}$

the tensile strength and fracture energy predictions by the two models (FPM and FPRM) with varying fiber length. Note that in the case of FPM the composite tensile strength (interpreted in this paper as the peak of the σ_B–δ relationship appropriate for pseudo strain hardening composite[2]) varies linearly with fiber length whereas in FPRM the fiber length does not have such a strong effect on tensile strength. Similarly in the case of FPRM as the fiber length increases there is more fiber rupture and less pullout and so the bridging stress drops much faster. Since fracture energy is computed as the area under the bridging stress crack opening curve, there is a decrease in fracture energy with increasing fiber length. Similar differences in composite property predictions between the two models can be observed if other parameters such as fiber diameter and interface bond strength are varied.

Prepeak σ_B–δ relationship

A typical σ_B–δ relationship resulting from the present analysis is shown in *Figure 8*. A physical explanation of the different events that transpire in the various sectors of crack opening is given in the following section. More detailed analytic expressions can be found in Appendix 4.

Sector A $(0 \le \delta \le (\delta_c)_1 e^{-f\pi})$. In this sector most of the fibers are in the debonding stage. Some fibers with extremely short embedment lengths are in the slipping stage. When the crack opening δ reaches $(\delta_c)_1 e^{-f\pi}$, all fibers of diameter d_1, $\phi = \pi/2$ with embedment length $\ell \ge (L_c)_1 e^{-f\pi/2}$ would rupture and the equations for $\sigma(\delta)$ or $\tilde{\sigma}(\tilde{\delta})$ governing sector A (Appendix 4) are no longer valid. $(\delta_c)_i$ is defined in terms of d_i by:

$$(\delta_c)_i = \frac{\sigma_{fu}^2 d_i}{4(1+\eta)E_f\tau} \qquad (i = 1, 2) \tag{12}$$

where $\eta = V_f E_f / V_m E_m$. Equation (12) also defines $(\delta_c)_2$ used in delimiting sector B.

Sector B $((\delta_c)_1 e^{-f\pi} \le \delta \le (\delta_c)_2 e^{-f\pi})$. Once $\delta \ge (\delta_c)_1 e^{-f\pi}$, fiber rupture becomes possible. Some fibers of $d_f \le d_f'$ (for which $\phi \ge \phi_1$, $\ell \ge L_c e^{-f\phi}$) have ruptured and no longer contribute to the bridging stress whereas fibers of $\ell < L_c e^{-f\phi}$ can debond and pullout. Fibers of $d_f > d_f'$ are still in the debonding/slipping stage as explained in sector A. Here

$$d_f' = \frac{4\delta E_f \tau(1+\eta)}{\sigma_{fu}^2 e^{-f\pi}}, \qquad \phi_1 = -\frac{1}{2f}\ln\left(\frac{E_f d_f \delta}{4L_c^2 \tau}\right) \tag{13}$$

At $\delta = (\delta_c)_2 e^{-f\pi}$ fibers of all diameters, with $\phi = \pi/2$ and embedment length $\ell \ge (L_c)_2 e^{f\pi/2}$ would rupture.

Sector C $((\delta_c)_2 e^{-f\pi} \le \delta \le (\delta_c)_1)$. In this sector, fibers of all diameters can rupture provided $\phi \ge \phi_1$ and $\ell \ge L_c e^{-f\phi}$. At $(\delta_c)_1$, fibers of diameter d_1 normal to the crack plane with $\ell \ge (L_c)_1$ can rupture.

Sector D $((\delta_c)_1 \le \delta \le (\delta_c)_2)$. This sector is similar to sector B in the sense that fibers of $d_f \le d_f''$ (for which $\ell \ge L_c e^{-f\phi}$) have ruptured. They have no debonding contribution. However fibers of $d_f > d_f''$ could still be in the stage characterized by sector C. At $(\delta_c)_2$, fibers of diameter d_2 normal to the crack plane with $\ell \ge (L_c)_2$ can rupture. Beyond $\delta > (\delta_c)_2$, there is no more fiber rupture. Only pullout of completely debonded fibers occurs. d_f'' is defined by:

$$d_f'' = \frac{4\delta E_f \tau(1+\eta)}{\sigma_{fu}^2} \tag{14}$$

Postpeak σ_B–δ relationship

Sector E $((\delta_c)_2 \le \delta \le (L_c)_1 e^{-f\pi/2})$. In this sector the bridging stress contribution comes from the pullout of those fibers that have not ruptured $(\ell < L_c e^{-f\phi})$. $(L_c)_i$ is defined as

$$(L_c)_i = \frac{d_i \sigma_{fu}}{4\tau} \qquad (i = 1, 2) \tag{15}$$

Sector F $((L_c)_1 e^{-f\pi/2} \le \delta \le (L_c)_2 e^{-f\pi/2})$. Beyond $\delta > (L_c)_1 e^{-f\pi/2}$, fibers of diameter d_1 and $\phi = \pi/2$ would have completely pulled out (fibers with longer embedment length would have ruptured) and will no longer contribute to crack bridging load. As δ continues to increase more and more fibers of larger diameter come under this category and hence their contributions would cease. For fibers of $d_f \le \hat{d}_f$ only those with $\phi < \phi_2$ can still pullout whereas for $d_f > \hat{d}_f$ fibers with the whole range of inclination angles can still pullout. Here:

$$\phi_2 = -\frac{1}{f}\ln\left(\frac{\delta}{L_c}\right), \qquad \hat{d}_f = \frac{4\tau\delta}{\sigma_{fu}} e^{f\pi/2} \tag{16}$$

Sector G $((L_c)_2 e^{-f\pi/2} \le \delta \le (L_c)_1)$. As $\delta > (L_c)_2 e^{-f\pi/2}$, fiber pullout could occur for fibers of all diameters. However only those fibers with $\phi < \phi_2$ would still be pulling out as fibers with $\phi \ge \phi_2$ would have completely pulled out.

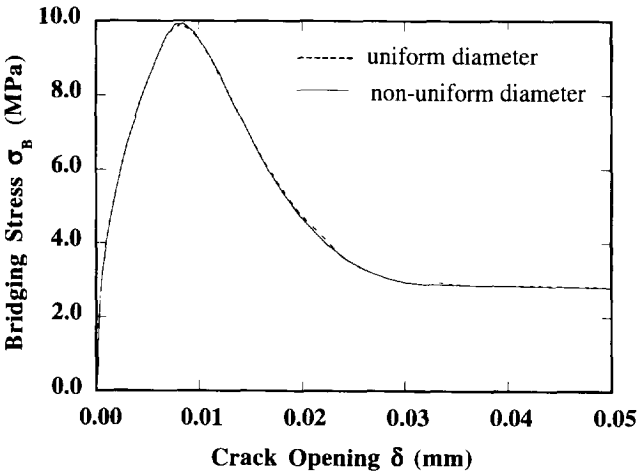

Figure 9 Influence of fiber diameter variation on the bridging stress crack opening relationship involving whole prepeak and portion of post-peak. This model allows for fiber rupture. Fiber parameters are $d_f^* = 25\,\mu$m, $\sigma = 1.25$ for the variable diameter case

Sector H $((L_c)_1 \leq \delta \leq (L_c)_2)$. As $\delta > (L_c)_1$, fibers with $d_f \leq \tilde{d}_f$ would have completely pulled out regardless of their inclination angle. Of the fibers with $d_f > \tilde{d}_f$ only those fibers with $\phi < \phi_2$ would still be pulling out. Here:

$$\tilde{d}_f = \frac{4\tau\delta}{\sigma_{fu}} \tag{17}$$

In the limiting case when d_1 and d_2 approach d_f^*, sectors B, D, F, and H vanish and the remaining sectors essentially recover the results derived for the uniform fiber diameter case of the FPRM model[4]. *Figure 9* shows the bridging-stress versus crack-opening relationship for a composite containing fibers with uniform diameter, $d_f^* = 25\,\mu$m, and that containing fibers with diameter varying between $d_1 = 20\,\mu$m and $d_2 = 30\,\mu$m with $\sigma = 1.25$. It can be seen that there is negligible change in the bridging stress for the composite containing varying fiber diameter as compared to that reinforced with fibers of uniform diameter only. Fracture energy and first crack strength comparisons between the mean and variable fiber diameter cases have not been carried out when fiber ruptures. However since the fracture energy and first crack strength are directly dependent on the σ_B–δ curve and since this curve remains essentially the same for the mean and varying fiber diameter cases one can expect that the fracture energy and first crack strength are not sensitive to fiber diameter variation.

DISCUSSION

To provide a feel of composite property magnitudes, computations are made for a composite with a specific set of fiber and interface parameters, given in *Table 1*. Composite properties have been predicted in *Table 2* by both the FPM and the FPRM, with and without fiber diameter variation. The fiber is assumed to be longer than critical fiber length $(2L_c e^{-f\pi/2})$. Two observations

Table 1 Fiber and interfacial parameters

E_f (GPa)	σ_{fu} (MPa)	τ (MPa)	d_f (mm)	L_f (mm)	
37	800	3	25 (20–30)	6	0.5

Table 2 Model predictions of composite properties

	FPM		FPRM	
	Fixed d_f	Variable d_f	Fixed d_f	Variable d_f
Tensile strength, σ_{cu} (MPa)	21.64	21.80	9.92	9.98
Fracture energy, G_c (N/mm)	21.64	21.80	1.20	1.21

can be drawn from these calculations: (1) fiber diameter distribution has negligible effect on composite properties whether fiber pulls out or ruptures: and (2) for the case where fiber ruptures the FPM could significantly overestimate the composite properties. The numerical values of the fracture energy and tensile strength are equal only for the particular fiber parameters chosen.

In order to bring out the effect of fiber diameter standard deviation on composite properties, the change in tensile strength and fracture energy are computed as a function of σ, for fixed $d_f^* = 10\,\mu$m, using the model with fiber pull-out only. *Figure 10* reveals that the tensile strength (peak bridging stress) rises with standard deviation. This is consistent for any d_f^* and the percentage increase in peak bridging stress for different d_f^* is identical provided σ/d_f^* is the same. For given d_f^* and standard deviation, the percentage increase in fracture energy and tensile strength is identical. This can be easily understood by comparing equations (8) and (10) where the percentage increase in composite properties for the variable diameter case over the uniform diameter case is given by the identical $k(z_1, z_2)$ term. The increase in composite properties can be attributed to the presence of smaller diameter fibers

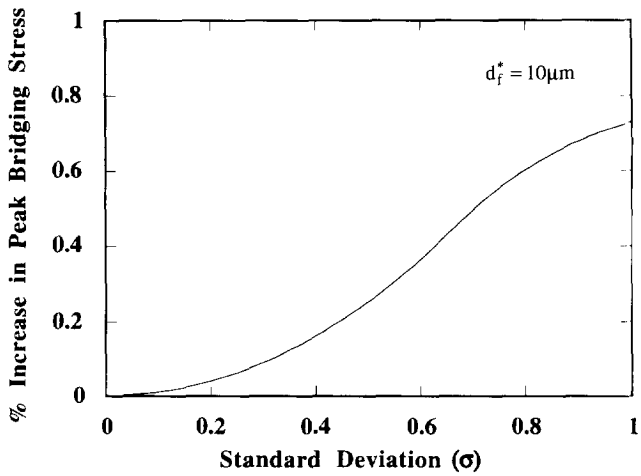

Figure 10 Effect of increasing standard deviation of fiber diameter (σ) on composite tensile strength, with $d_f^* = 10\,\mu$m

which have a higher reinforcement efficiency. The non-linear relationship between composite properties and fiber diameter causes an incomplete cancellation effect between small and large diameter fibers, with a net gain, albeit small, in composite properties.

The slight increase in composite properties due to varying fiber diameter is only of theoretical interest. Practically that change may not be noticeable due to experimental variations. But the main aspect that is to be observed is that there is no property deterioration. This indicates that fiber diameter control can be relaxed without affecting composite properties.

The normal probability distribution is assumed to describe the variation of fiber diameter because it is the most common type of continuous probability distribution. If a uniform probability density function is assumed it is observed that the increase in properties is even better. But considering that actual measurement of fiber diameter variation[6] indicates a normal probability distribution, the assumption adopted seems reasonable.

Fiber length variation could also influence composite properties. A theoretical and experimental study of this problem has been carried out by Li and Obla[9]. Contrary to diameter distribution, length distribution can be caused during fiber manufacture, handling and composite processing and has a sizable negative effect on composite properties.

CONCLUSIONS

1. There is a negligible change in composite strength and toughness due to fiber diameter variation according to a normal probability distribution. This suggests that the relaxation of fiber diameter control will not cause deterioration in properties of cementitious composites. The above conclusion is true for any mean fiber diameter considered.
2. The theoretical conclusion that non-uniform fiber diameter does not affect composite properties holds true whether the fiber pulls out or ruptures.

This study represents an investigation of the acceptability of manufactured fiber diameter variation only given that fiber diameters do vary for almost any given fiber type. This study is not directed towards optimizing composite properties. In other words it is not a recommendation that large fiber diameter distribution should be sought for. Rather, this study concludes that non-uniform fiber diameter resulting from manufacturing processes do not necessarily translate into composite property deterioration.

ACKNOWLEDGEMENTS

This research has been partially supported by a grant from the Conoco Inc., and a grant from the National Science Foundation (BCS 9202097) to the University of Michigan, Ann Arbor, MI. Helpful discussions with Dr J. McConaghy are gratefully acknowledged.

REFERENCES

1 Li, V.C. Post-crack scaling relations for fiber reinforced cementitious composites. *ASCE J. Mater. Civil Eng.* 1992, **4**, 41
2 Li, V.C. and Leung, C.K.Y. Theory of steady state and multiple cracking of random discontinuous fiber reinforced brittle matrix composites. *ASCE J. Eng. Mech.* 1992, **118**, 2246
3 Marshall, D.B. and Cox, B.N. A *J*-integral method for calculating steady-state matrix cracking stresses in composites. *Mech. Mater.* 1988, **7**, 127
4 Maalej, M., Li, V.C. and Hashida, T. Effect of fiber rupture on tensile properties of short fiber composites. *ASCE J. Eng. Mech.* 1994, **121**, 903
5 Li, V.C., Wang, Y. and Backer, S. A micromechanical model of tension softening and bridging toughening of short random fiber reinforced brittel matrix composites. *J. Mech. Phys. Solids* 1991, **39**, 607
6 Brown, S.E. Characterization of the fiber diameter distributions of synthetic mineral fiber products and their dusts. *American Industrial Hygiene Association* 1992, **53**, 27
7 Li, V.C., Wang, Y. and Backer, S. Effect of inclining angle, bundling, and surface treatment on synthetic fiber pull-out from a cement matrix. *Composites* 1990, **21**, 132
8 Rice, J.R. Mathematical analysis in the mechanics of fracture, in 'Fracture –An Advanced Treatise', Vol. 2 (Ed. H. Liebowitz), Academic Press, 1968, pp. 191–311
9 Li, V.C. and Obla, K. Effect of fiber length variation on tensile properties of carbon fiber cement composites. *Int. J. Composites Eng.* 1994, **4**, 947
10 Morton, J. and Groves, G.W. The effect of metal wires on the fracture of a brittle matrix composite. *J. Mater. Sci.* 1976, **11**, 617

APPENDIX 1: EXPRESSIONS FOR COMPOSITE PROPERTIES FOR THE CASE WITH UNIFORM FIBER DIAMETER

The fiber pull-out load P has been related to the pull-out displacement δ based on a constant frictional interface bond strength (τ)[1]:

$$P(\delta;\phi) = \begin{cases} \frac{\pi}{2}(E_f d_f^3 \tau\delta)^{1/2} e^{f\phi} \equiv P_1(\delta;\phi) & \text{for } \delta \le \delta_0 \\ \pi\tau\ell d_f[1-(\delta-\delta_0)/\ell]e^{f\phi} \equiv P_2(\delta;\phi) & \text{for } \ell \ge \delta \ge \delta_0 \end{cases} \quad \text{(A1)}$$

where $\delta_0 \equiv 4\ell^2\tau/E_f d_f$ corresponding to full debonding of the fiber, and E_f, L_f, l, and d_f are fiber modulus, length, embedded length and diameter, respectively.

The factor $e^{f\phi}$ corresponds to the snubbing effect due to inclined fiber pullout[7,10], where ϕ is the angle made by the fiber with the loading axis and f is the snubbing coefficient.

Using equation (1) but without the fiber diameter variation term (i.e. setting $p_1(d_f)$ to a Delta function) and employing equation (A1) for the $P(\delta;\phi)$ term, Li[1] derived the prepeak $\tilde{\sigma}_B(\tilde{\delta})$ relationship as

$$\tilde{\sigma}_B(\tilde{\delta}) = g[2(\tilde{\delta}/\tilde{\delta}^*)^{1/2} - \tilde{\delta}/\tilde{\delta}^*] \text{ for } \tilde{\delta} \le \tilde{\delta}^* \quad \text{(A2)}$$

where $\tilde{\sigma}_B = \sigma_B/\sigma_0$, $\sigma_0 = V_f\tau(L_f/d_f^*)/2$, $\tilde{\delta} = \delta/(L_f/2)$ and $\tilde{\delta}^* = 2(\tau/E_f)(L_f/d_f^*)$.

The snubbing factor g is defined in terms of the snubbing coefficient f:

$$g = \frac{2}{4+f^2}(1+e^{\pi f/2})$$

Similarly the post-peak $\tilde{\sigma}_B(\tilde{\delta})$ relationship is found to be

$$\tilde{\sigma}_B(\tilde{\delta}) = g(1-\tilde{\delta})^2 \quad \text{for } 1 \geq \tilde{\delta} \geq \tilde{\delta}^* \tag{A3}$$

and the composite fracture energy due to fiber pull-out is shown to be

$$G_c = \frac{1}{12} g\tau V_f d_f \left(\frac{L_f}{d_f}\right)^2 \tag{A4}$$

Balancing the combined stress intensity factor due to applied remote loading K_L and that due to fiber bridging behind the crack tip K_B, with the crack tip fracture toughness K_{tip} requires:

$$K_L + K_B = K_{tip} \tag{A5}$$

where $K_{tip} = (E_c/E_m)K_m$, K_m = matrix fracture toughness, E_c and E_m are composite and matrix toughness respectively. The normalized stress intensity factor due to ambient tensile loading σ is given as

$$\tilde{K}_L = 2\sqrt{\frac{\tilde{c}}{\pi}}\,\tilde{\sigma} \tag{A6}$$

and the normalized stress intensity factor due to fiber bridging is given by

$$\tilde{K}_B = -2\sqrt{\frac{\tilde{c}}{\pi}} \int_0^1 \tilde{\sigma}_B(\tilde{\delta}) \frac{R}{\sqrt{1-R^2}} dR \tag{A7}$$

where R takes a numerical value between 0 and 1 depending on where one is located along the crack flanks with 0 corresponding to the center of the crack opening and 1 the crack tip.

Combining these results, Li and Leung[2] calculated the normalized first crack strength $\tilde{\sigma}_{fc}$ as a function of the normalized crack size $\bar{c}$ as follows:

$$\frac{\tilde{\sigma}_{fc}}{g} = \frac{\sqrt{\pi}}{2}\frac{\bar{K}}{\bar{c}} + \left(\frac{4}{3}\sqrt{\bar{c}} - \frac{1}{2}\bar{c}\right) \tag{A8}$$

where

$$\bar{K} \equiv \left(\frac{K_{tip}}{\sigma_0\sqrt{c_0}}\right)/g\tilde{\delta}^*, \qquad \bar{c} \equiv \sqrt{\tilde{c}}/\tilde{\delta}^*, \qquad \tilde{c} = c/c_0,$$

$$c_0 \equiv \left(\frac{L_f E_c}{2K_{tip}}\right)^2 \frac{\pi}{16(1-\nu^2)^2}$$

and c = critical crack size.

APPENDIX 2: DERIVATION OF PREPEAK σ_B–δ RELATIONSHIP FOR VARIABLE FIBER DIAMETER COMPOSITE

Equation (1) may be written in the form

$$\sigma_B(\delta) = \frac{4V_f}{\pi}\int_{d_1}^{d_2}\int_0^{\pi/2}\int_0^{z_0\cos\phi}\frac{1}{d_f^2} \times P(\delta;\phi)\sin\phi p(d_f)dz'\,d\phi\,dd_f \tag{A9}$$

where $z' = z/(L_f/2)$. The prepeak part of the σ_B–δ curve ($\tilde{\delta} \leq \tilde{\delta}^*$) has contributions from two groups of fibers — debonding and slipping fibers with $P(\delta;\phi)$ described by equation (A1). Fibers in the first group pass into the second group as δ increases.

For $\tilde{\delta} \leq \tilde{\delta}_2$:

$$\sigma_B(\delta)|_{debond} = \frac{4V_f}{\pi}\int_{d_1}^{d_2}\int_0^{\pi/2}\int_0^{z_0\cos\phi}\frac{1}{d_f^2}P_1(\delta;\phi) \times \sin\phi p(d_f)dz'\,d\phi\,dd_f \tag{A10}$$

$$\sigma_B(\delta)|_{slipping} = \frac{4V_f}{\pi}\int_{d_1}^{d_2}\int_0^{\pi/2}\int_0^{(1-\tilde{\delta})\cos\phi}\frac{1}{d_f^2}P_2(\delta;\phi) \times \sin\phi p(d_f)dz'\,d\phi\,dd_f \tag{A11}$$

where $P_1(\delta;\phi)$ and $P_2(\delta;\phi)$ are given by the first and second terms of equation (A1) respectively and

$$z_0 = 1 - \left(\frac{E_f d_f \tilde{\delta}}{2\tau L_f}\right)^{1/2}$$

By combining these two contributions and normalizing σ_B and δ we can simplify it to equation (7a).

For $\tilde{\delta}_2 \leq \tilde{\delta} \leq \tilde{\delta}_1$, let us choose a point $\tilde{\delta} = 2(\tau/E_f)(L_f/d_f')$ where $d_1 \leq d_f' \leq d_2$. At this point, (1) fibers of diameter $d_f \geq d_f'$ are in the complete slipping stage, and (2) fibers of diameter $d_f \leq d_f'$ are still in the debonding/pullout stage.

Thus

$$\sigma_B(\delta) = \frac{4V_f}{\pi}\left\{\begin{aligned}&\int_{d_1}^{\tau L_f E_f\tilde{\delta}}\int_0^{\pi/2}\int_0^{z_0\cos\phi}\frac{1}{d_f^2}P_1(\delta;\phi) \times \sin\phi p(d_f)dz'\,d\phi dd_f \\ &+\int_{d_1}^{\tau L_f/E_f\tilde{\delta}}\int_0^{\pi/2}\int_{z_0\cos\phi}^{(1-\tilde{\delta})\cos\phi}\frac{1}{d_f^2}P_2(\delta;\phi) \times \sin\phi p(d_f)dz'\,d\phi dd_f \\ &+\int_{\tau L_f/E_f\tilde{\delta}}^{d_2}\int_0^{\pi/2}\int_0^{(1-\tilde{\delta})\cos\phi}\frac{1}{d_f^2}P_2(\delta;\phi) \times \sin\phi p(d_f)dz'\,d\phi dd_f\end{aligned}\right\} \tag{A12}$$

Solving and normalizing we obtain equation (7b).

Note that, though the actual peak of the σ_B–δ curve is reached slightly before $\tilde{\delta}_2$, for terminology we call the region till $\tilde{\delta}_1$ as the prepeak part of the curve. In the limiting case when d_1 and d_2 approach d_f^* (i.e. fibers with uniform diameter d_f^*), equation (7b) vanishes as $\tilde{\delta}_1$ becomes equal to $\tilde{\delta}_2$. However equation (7a) reduces to equation (A2) as $h(z_1, z_2)$ tends to unity. Thus when the fiber diameter is assumed to be uniform, the original results of prepeak σ_B–δ relationship (equation (A2)) reported in Li[1] are recovered. At $\tilde{\delta} = \tilde{\delta}_2$, the third term in equation (7b) vanishes and equations (7a) and (7b) become identical as the $\tilde{\sigma}_B(\tilde{\delta})$ curve is continuous. These checks are also carried out for the post-peak bridging stress crack opening relationship, fracture energy and first crack strength.

APPENDIX 3: DERIVATION OF COMPOSITE FIRST CRACK STRENGTH FOR VARIABLE FIBER DIAMETER COMPOSITE

Referring to Li and Leung[2], balancing the stress intensity factor gives

$$K_L + K_B = K_{tip}$$
$$\tilde{K}_B = \frac{K_B}{\sigma_0\sqrt{c_0}} = -2\frac{\sqrt{\tilde{c}}}{\pi}\int_0^1 \tilde{\sigma}_B(\tilde{\delta})\frac{R}{\sqrt{1-R^2}}dR \qquad \text{(A13)}$$

where $\tilde{\sigma}_B(\tilde{\delta})$ corresponds to the prepeak part of the bridging stress crack opening curve only. Also, $\tilde{c} = c/c_0$, $\bar{c} = \sqrt{\tilde{c}}/\tilde{\delta}^*$, $\tilde{\delta} = \sqrt{\tilde{c}(1-R^2)}$ and R is a normalized crack length parameter that takes the value 0 at the center of the elliptical crack and 1 at the edge.

For $\bar{c} \le d_f^*/d_2$, $(\tilde{\delta})_{max} \le \tilde{\delta}_2$ where $(\tilde{\delta})_{max}$ is the maximum crack width at the center of the crack and so all $(\tilde{\delta})$ along the crack is less than $\tilde{\delta}_2$. This leads to the first crack strength expression in equation (11a).

For $d_f^*/d_2 \le \bar{c} \le d_f^*/d_1$ we have two cases: (i) for $0 \le R \le a$; $\tilde{\delta}_2 \le \tilde{\delta} \le \tilde{\delta}_1$ and the portion of the prepeak $\tilde{\sigma}_B$–$\tilde{\delta}$ curve (equation (7b)) that satisfies this $\tilde{\delta}$ is used; (ii) for $a \le R \le 1$; $\tilde{\delta} \le \tilde{\delta}_2$ and the portion of the prepeak $\tilde{\sigma}_B$–$\tilde{\delta}$ curve, (equation (7a)) that satisfies this $\tilde{\delta}$ is used. a is defined by $a = [1 - (d_f^*/d_2\bar{c})^2]^{1/2}$. Combining these two contributions we obtain equation (11b).

APPENDIX 4: COMPLETE σ_B–δ RELATIONSHIP FOR THE CASE WHERE FIBER CAN RUPTURE AND HAS DIAMETER DISTRIBUTION

Referring to *Figure 8*, the σ_B–δ relationship in the various sectors with corresponding δ ranges are given in *Table A1*, where

$$k_1(a,b,c,d,x,y) = \frac{4V_f}{\pi}\int_a^b\int_c^d\int_x^y \frac{1}{d_f^2}P_1(\delta;\phi) \times \sin\phi p(d_f)dz'd\phi dd_f$$

$$k_1(a,b,c,d,x,y) = \frac{4V_f}{\pi}\int_a^b\int_c^d\int_x^y \frac{1}{d_f^2}P_2(\delta;\phi) \times \sin\phi p(d_f)dz'd\phi dd_f$$

$$\hat{z}_0 = z_0\cos\phi, \qquad \hat{z}_1 = \cos\phi, \qquad h = \left(1 - \frac{2\delta}{L_f}\right)\cos\phi$$
$$\hat{z}_1 = \left(1 - \frac{2L_c}{L_f}e^{-f\phi}\right)$$

After simplification and appropriate normalization, one obtains the values given in *Table A2*, where

$$\hat{\delta} = \frac{\tilde{\delta}}{\bar{\delta}}, \quad \bar{\delta} = \left(\frac{2\tau}{(1+\eta)E_f}\right)\left(\frac{L_f}{d_f}\right),$$

$$\hat{L}_c = \frac{2L_c}{L_f}, \qquad c(x,y) = \int_x^y [2(\hat{\delta})^{1/2} - \hat{\delta}]p_3(d_f)dd_f$$

Table A1

Sector	$\sigma(\delta)$	δ range
A	$k_1(d_1,d_2,0,\pi/2,0,\hat{z}_0) + k_2(d_1,d_2,0,\pi/2,\hat{z}_0,h)$	$0 \le \delta \le (\delta_c)_1 e^{-f\pi}$
B	$k_1(d_f',d_2,0,\pi/2,0,\hat{z}_0) + k_2(d_f',d_2,0,\pi/2,\hat{z}_0,h) + k_1(d_1,d_f',0,\phi_1,0,\hat{z}_0) - k_2(d_1,d_f',0,\phi_1,\hat{z}_0,h)$ $-k_2(d_1,d_f',\phi_1,\pi/2,\hat{z}_1,h)$	$(\delta_c)_1 e^{-f\pi} \le \delta \le (\delta_c)_2 e^{-f\pi}$
C	$k_1(d_1,d_2,0,\phi_1,0,\hat{z}_0) + k_2(d_1,d_2,0,\phi_1,\hat{z}_0,h) + k_2(d_1,d_2,\phi_1,\pi/2,\hat{z}_1,h)$	$(\delta_c)_2 e^{-f\pi} \le \delta \le (\delta_c)_1$
D	$k_1(d_f'',d_2,0,\phi_1,0,\hat{z}_0) - k_2(d_f'',d_2,0,\phi_1,\hat{z}_0,h) + k_2(d_f'',d_2,\phi_1,\pi/2,\hat{z}_1,h) + k_2(d_1,d_f'',0,\pi/2,\hat{z}_1,h)$	$(\delta_c)_1 \le \delta \le (\delta_c)_2$
E	$k_2(d_1,d_2,0,\pi/2,\hat{z}_1,h)$	$(\delta_c)_2 \le \delta \le (L_c)_1 e^{f\pi/2}$
F	$k_2(\hat{d}_f,d_2,0,\pi/2,\hat{z}_1,h) + k_2(d_1,\hat{d}_f,0,\phi_2,\hat{z}_1,h)$	$(L_c)_1 e^{-f\pi/2} \le \delta \le (L_c)_2 e^{-f\pi/2}$
G	$k_2(d_1,d_2,0,\phi_2,\hat{z}_1,h)$	$(L_c)_2 e^{-f\pi/2} \le \delta \le (L_c)_1$
H	$k_2(\hat{d}_f,d_2,0,\phi_2,\hat{z}_1,h)$	$(L_c)_1 \le \delta \le (L_c)_2$

Table A2

Sector	$\bar{\sigma}(\hat{\delta})$	Range
A	$gc(d_1,d_2)$	$0 \le \delta \le (\delta_c)_1 e^{-f\pi}$
B	$gc(d_f',d_2) + d(d_1,d_f') + e(d_1,d_f')$	$(\delta_c)_1 e^{-f\pi} \le \delta \le (\delta_c)_2 e^{-f\pi}$
C	$d(d_1,d_2) + e(d_1,d_2)$	$(\delta_c)_2 e^{-f\pi} \le \delta \le (\delta_c)_1$
D	$d(d_f'',d_2) + e(d_f'',d_2) + f(d_1,d_f'')$	$(\delta_c)_1 \le \delta \le (\delta_c)_2$
E	$f(d_1,d_2)$	$(\delta_c)_2 \le \delta \le (L_c)_1 e^{f\pi/2}$
F	$f(\hat{d}_f,d_2) + g(d_1,\hat{d}_f)$	$(L_c)_1 e^{-f\pi/2} \le \delta \le (L_c)_2 e^{-f\pi/2}$
G	$g(d_1,d_2)$	$(L_c)_2 e^{-f\pi/2} \le \delta \le (L_c)_1$
H	$g(\hat{d}_f,d_2)$	$(L_c)_2 \le \delta \le (L_c)_2$

$$d(x,y) = \int_x^y g(\phi_1)[2(\hat{\delta})^{1/2} - \hat{\delta}]\, p_3(d_f)\mathrm{d}d_f,$$

$$e(x,y) = \int_x^y a(-f)\hat{L}_c^2 p_3(d_f)\mathrm{d}d_f$$

$$f(x,y) = \int_x^y [g_1\hat{L}_c^2 - 2\hat{L}_c + g\hat{\delta}^2]\, p_3(d_f)\mathrm{d}d_f$$

$$g(x,y) = \int_x^y [d(-f)\hat{L}_c^2 - 2d(0)\hat{L}_c\hat{\delta} + d(\mathrm{f})\hat{\delta}^2]p_3(d_f)\mathrm{d}d_f$$

$$g(\phi_1) = \frac{1}{(4+f^2)}\{[f\sin(2\phi_1) - 2\cos(2\phi_1)]\mathrm{e}^{f\phi_1} + 2\}$$

$$a(t) = \frac{1}{(4+t^2)}\{[2\cos(2\phi_1) - t\sin(2\phi_1)]\mathrm{e}^{t\phi_1} + 2\mathrm{e}^{t\pi/2}\}$$

$$d(t) = \frac{1}{(4+t^2)}\{[t\sin(2\phi_2) - 2\cos(2\phi_2)]\mathrm{e}^{t\phi_2} + 2\}$$

$$g_1 = \frac{2}{(4+f^2)}[1 + \mathrm{e}^{-f\pi/2}]$$

At values of δ that separates adjacent sectors, it can be verified that the bridging stress from both sectors as given in the table above match. No jumps in the σ_b -δ relationship are expected.